PCM Thermal Storage System Analysis Using EnergyPlus and BCVTB

Aidan Jones and Donal Finn
School of Mechanical and Materials Engineering
University College Dublin, Ireland

Abstract

This paper presents the implementation of a phase change material thermal storage unit in EnergyPlus and an analysis of the energy cost of its use in a retrofit application. A significant portion of the daily electrical heating load can be shifted from on-peak to off-peak times if flexibility is brought to heating loads by methods such as thermal storage. In this paper it is seen that use of the thermal storage system increases overall electrical use over the course of a 24 hour period. A time of use price incentive or tariff dependent on load management would be necessary to facilitate the adoption of such demand side management technology. The analysis is performed using a comprehensive phase change material thermal storage model, developed using Matlab, which is validated in this paper. This model is incorporated into the EnergyPlus environment through the Building Controls Virtual Test Bed. The rest of the plant is modelled in EnergyPlus, using equipment specifications from a retrofit application of an office building.

1 Introduction

As the renewable energy sector continues to rise in importance in the context of many national electric grids, the integration of these often unpredictable energy sources, in particular wind, becomes increasingly challenging. Building energy use for heating and cooling applications constitutes a significant proportion of national electricity demand. Thermal energy storage offers a method of shifting building load away from times of high grid demand to times of low demand. Phase change materials (PCM) thermal storage tanks make use of high latent heat capacities to store thermal energy at almost isothermal conditions, enabling high density energy storage and robust heat transfer fluid (HTF) supply temperatures.

In general, load shifting has positive effects on the electrical load profile of buildings; such demand side management schemes would be welcomed by utilities. Such strategies must, however, be assessed under both economic and energy consumption considerations. In this paper, relevant previous work is introduced and a mathematical model of the thermal system is described, including its validation and implementation in the EnergyPlus environment through use of the Building Controls Virtual Test Bed (BCVTB). The performance of the active hot thermal storage system is assessed and the implications of these results discussed and conclusions drawn.

2 Literature Review

There is a significant volume of previous work in the area of thermal storage simulation. Much of the focus has been on building thermal storage models for various configurations. A small number of research papers have been concerned with PCM encapsulated in flat blocks.

A fraction of these investigated a liquid HTF, with others considering air as the working fluid. Liu et al. (2011) modelled a PCM tank for cooling applications consisting of horizontally stacked encapsulation plates and validated against results from their experimental setup. The experimental results from this paper were used for validation of a TRYNSYS model by D'Avignon and Kummert (2012), developed for heating applications. Elsayed (2007) constructed a model to analyse the effects of cyclic charging of a PCM tank, with validation performed against data from Chang-Yong and Hsieh (1992). Few PCM TSU models are incorporated into full system models for integrated system analysis. Ihm et al. (2004) introduced an ice thermal storage system into EnergyPlus. Much of the work on whole system analysis has involved tiered pricing structures. Henze et al. (1997) investigated four rate structures for four operation modes to assess cooling load shifting, including chiller and pump power consumption for ice storage systems. There have been several studies on combined active and passive storage using optimal control and tiered pricing including Kintner-Meyer and Emery (1995), Henze et al. (2004), Hajiah and Krarti (2012a, 2012b).

The aim of this paper is to take a detailed, system-wide, approach to PCM thermal storage unit (TSU) integration into a complete plant system, including pumps fans, buffer tank and ground source heat pump (GSHP), as well as a comprehensive building model. This paper describes a novel method of modelling a PCM TSU in EnergyPlus and unlike the work above, is analysed in conjunction with a GSHP.

3 System Description

Figure 1: Demonstration site located at Coimbra, Portugal

The retrofit system under consideration as a test bed for this work is a demonstration site located in Coimbra, Portugal (Figure 1), which is part of the European Union FP7 GROUNDMED project (www.groundmed.eu). The building in question is thermally massive, allowing further studies on passive thermal energy storage. The third floor of the building is modelled in this study and is used for municipal offices, with a plan area of 586 m^2. Coimbra is located approximately 40 km inland from the Atlantic coast. The plant layout is described in Figure 2; the hydronic circuit consists of a ground loop and two decoupled internal loops, driven by three variable speed pumps. The decoupled nature of the loops means that the two internal loops can operate somewhat independently, allowing more scope for advanced control. The primary loop pump has a maximum power rating of 430 W, the secondary loop pump and external loop pump are rated at 800 W. The buffer tank has a volume of 1,000 li-

tres. The secondary loop supplies hot water to heat the building spaces; a total of 33 fan coil units meet the heating loads in each of the twenty conditioned spaces, which can exceed 250 kWh per day, with a peak heating load of over 50 kW.

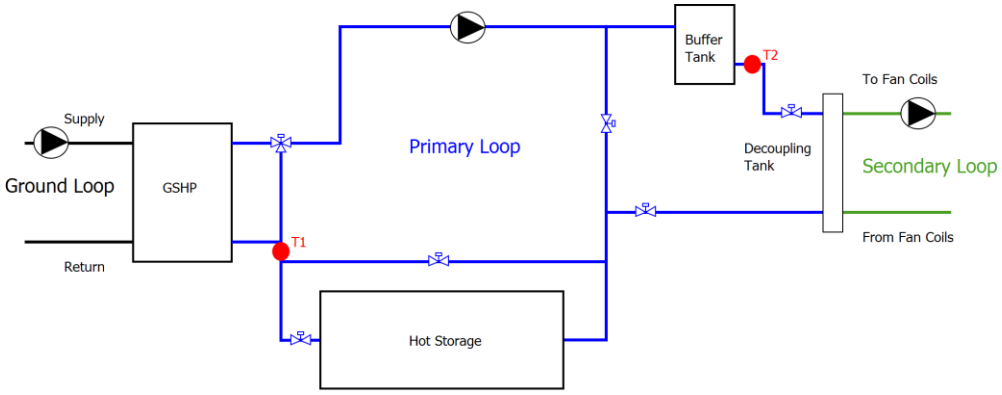

Figure 2: Hydronic system schematic

Thermal Storage Unit

The hot thermal storage unit installed onsite has a capacity of 100 kWh. Such a large tank capacity means that a significant level of flexibility can be brought into the building heating load. It uses a salt hydrate PCM with a melting temperature of 46 °C. The PCM is encapsulated in flat rectangular containers, stacked vertically (Figure 3), with 18 slabs running the length of the tank, consisting of smaller containers fixed together. Water is used as the heat transfer fluid and flows between the surfaces of the PCM slabs. The total tank volume is 2 m^3, with a volumetric water content of 40%.

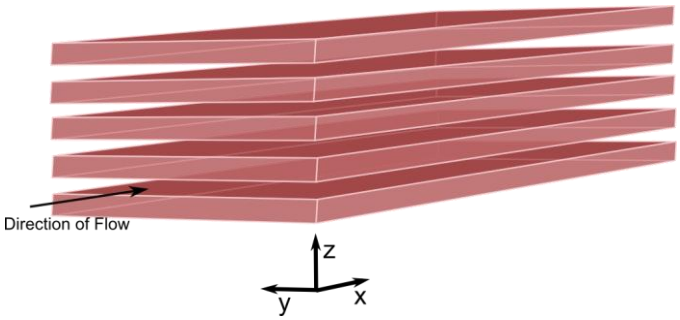

Figure 3: PCM tank layout

GSHP

The ground source heat pump is a tandem compressor unit with a heating capacity of 70.4 kW and a cooling capacity of 61.5 kW at supply/return water temperatures of 45/40 °C and 7/12 °C, respectively. The rated COP is 4.73 for cooling and 4.29 for heating. The ground heat exchanger consists of seven vertical boreholes with water as the working fluid.

4 Modelling Methodology

EnergyPlus

EnergyPlus is used in this project to model the building and HVAC system. The overall aim of the project is to develop algorithms aimed at optimising the deployment of active storage inventories and the effective use of the passive storage due to the presence of a high thermal mass in the analysed building. The presence of significant thermal mass is particularly common in older retrofit applications. In the case of this work, EnergyPlus is used to model the performance of the building fabric, the effect of occupancy and equipment on building loads, the fan coils in the conditioned spaces, as well as the detailed plant and the hydronic circuit. To assess the effectiveness of the PCM TSU, it cannot be modelled in isolation; it must be modelled as part of an entire system, including the equipment used to charge and discharge it, i.e., GSHP, internal primary and external circulation pumps. The building model is essential to analyse the performance of the system under real-life constraints from a comfort and load point of view.

PCM TSU Model

This model was introduced previously in Jones and Finn, (2013); in the current paper it is validated and used as a key component in the simulation work. The model uses an explicit forward finite difference method. Uniform flow distribution is assumed across the HTF passages formed by the parallel plates; the entry or exit regions are not modelled. Table 1 summarises the key properties of the PCM TSU used in the current system:

Table 1: PCM Tank Properties

Thermal Energy Capacity	100 kWh (latent)
PCM	Salt Hydrate
PCM Melting Temperature	46 ºC
Mass of PCM	1,895 kg
Thickness of PCM slabs	0.03 m
Vertical gap between capsules	0.01 m
PCM Latent Heat of Fusion	190 $kJ \cdot kg^{-1}$
PCM Specific Heat Capacity	2.41 $kJ \cdot kg^{-1} \cdot K^{-1}$
PCM Thermal Conductivity	0.45 $W \cdot m^{-1} \cdot K^{-1}$
Tank dimensions (x,y,z)	3.5 m x 0.75 m x 0.75 m

The PCM tank model is based on the following assumptions:

- Constant HTF properties.
- Constant PCM properties within one phase.
- One dimensional heat transfer.
- No PCM hysteresis or subcooling.
- No heat loss through the shell of the tank.
- No heat is absorbed by the capsules or tank shell.

The length of the tank is sub-divided into control volumes along the x axis. For each control volume and timestep, the heat transfer is calculated, resulting in a change in PCM temperature or liquid fraction. A resistance network is set up between the PCM and the HTF, including convection resistance due to water-shell interface and conduction resistances due to the capsule material and presence of charged PCM. The conduction resistance of the charged PCM increases as the latent capacity of the tank is charged, as in Equation 1, where k_{PCM} is the conductivity of the PCM resisting heat transfer, t_{PCM} is the thickness of the charged layer and A is the surface area of the node.

$$R_{cond,PCM} = \frac{t_{PCM}}{k_{PCM} A} \quad (1)$$

The convection resistance is calculated using a Nusselt number (Nu) correlation in Equation 2, (Shah and London, 1978) and Equation 3.

$$Nu_{x,T} = \begin{cases} 1.233(x^*)^{-\frac{1}{3}} + 0.4, & x^* \leq 0.001 \\ 7.541 + 6.874(10^3 x^*)^{-0.488} e^{-245x^*}, & x^* < 0.001 \end{cases} \quad (2)$$

$$R_{conv} = D_h / Nu \cdot k_{water} \cdot A \quad (3)$$

where $x^* = \left(\frac{x}{Dh}\right) / (Re \cdot Pr)$, x is distance from the inlet, Re is Reynolds number and Pr is Prandtl number, D_h is the hydraulic diameter and k_{water} is the thermal conductivity of the HTF.

Model Integration with EnergyPlus

Once the model was set up for real time simulation, it was connected as a component in EnergyPlus. This was achieved by using the *PlantComponent:UserDefined* EnergyPlus module and the Building Controls Virtual Test Bed (BCVTB).

BCVTB

The BCVTB is a middleware software utility which allows communication between multiple simulation programs including: Modelica, EnergyPlus, Simulink, Matlab. EnergyPlus and Matlab are called as clients of the BCVTB. The configuration file defines the EnergyPlus data exchange: source and destination of the shared variables. Data is made available from EnergyPlus through the *Output:Variable* object; inputs are read through the *ExternalInterface* facility. In Matlab, data exchange is handled as an input and an output array. The *Ptolemy II* graphical user interface allows for connection of the two programs and simulation runs. In this case, the BCVTB initialises the transfer, EnergyPlus outputs the TSU inlet water flow rate and temperature; Matlab outputs the outlet water temperature, state of charge and heat transfer rate.

Validation

Validation of any mathematical model is important to ensure it accuracy. It is also important for troubleshooting and fine tuning a model. It was expected that measurement data from the on-site installation would be available by the time of writing, but operational constraints resulted in delays in installation. The model is, however, validated against data from the literature (Liu et al., 2011). This study by Liu et al. was chosen because it makes use of stacked flat plates to encapsulate the PCM and it uses a water-based heat transfer fluid. To validate the present model against this data set, all possible input parameters were changed to match those

present in the experimental setup, while maintaining the core simulation engine. The thesis from which this research is based was also used a source of information (Liu, 2010).

A significant design difference exits between the two tanks is their size: 100 kWh (360 MJ) at Coimbra compared to 6.25 kWh (22.5 MJ) for the work of Liu et al. The present model is scalable and can easily adapt to new physical parameters. The other difference is the end use: cooling versus heating. Fundamentally, the assumptions made in the model render these differences less important than would be expected. Heat transfer is driven by a finite temperature difference and it is assumed that there are no heat losses; the tank used in the study by Liu et al. is insulated. The thermophysical attributes of the HTF and PCM were inserted into the present model and the direction of heat flow is dealt with by the model without alteration.

The model tank in the cited paper consists of 19 parallel flat slabs, 1.7 m x 0.26 m x 0.025 m with a 0.006 m gap between these plates. These physical attributes were changed, as were the properties of the HTF – from water to an ethylene glycol solution. The properties of the PCM were also changed to match the experiment – density, phase change temperature and latent heat of fusion. An entrance and exit region of length 0.5 m was added at each end of the PCM capsules for HTF diffusion. These are modelled as well-mixed bodies of water.

Two sets of experimental data are available from Liu et al.: the inlet and outlet temperatures from two discharge tests. Figure 4 and Figure 5 compare the predicted tank outlet temperatures from the present model against experimental data for two tests: flow rates of 0.22 $l \cdot s^{-1}$ and 0.32 $l \cdot s^{-1}$, respectively.

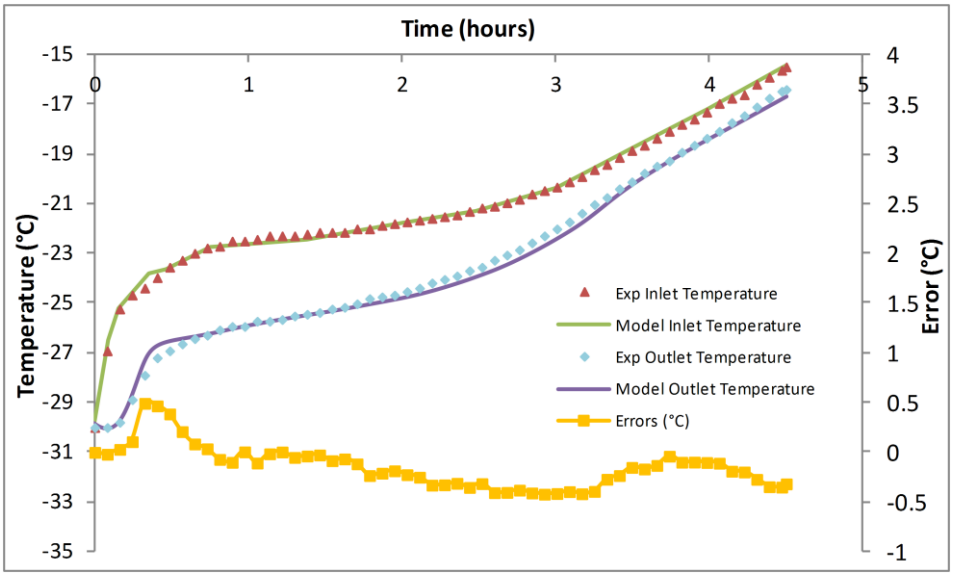

Figure 4: Modelled, experimental outlet temperature (0.22 $l \cdot s^{-1}$) and error

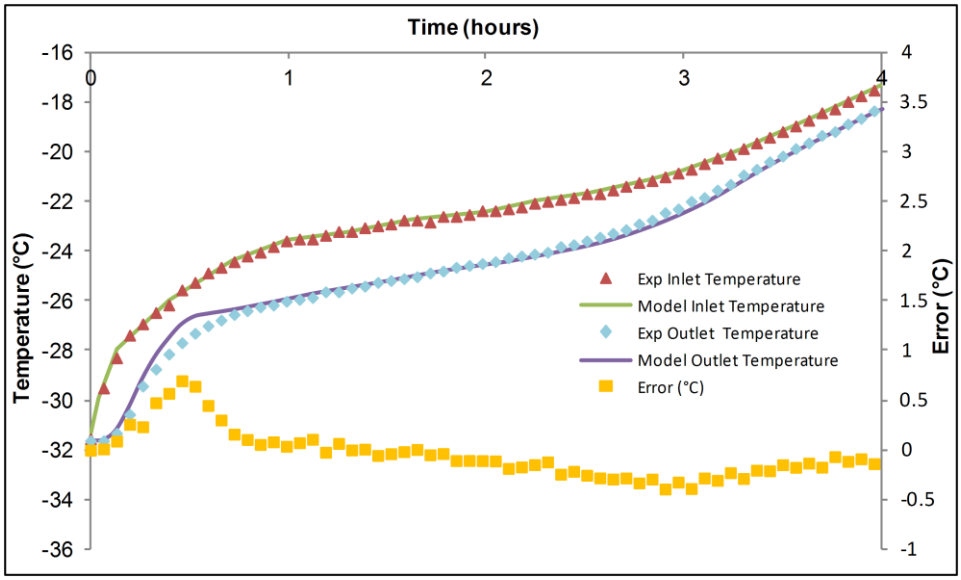

Figure 5: Modelled, experimental outlet temperature and error (0.32 l·s^{-1})

These figures also illustrate the error in °C between the outlet temperature from the model and the experimental results. As can be seen from the above figures, the model performs well in both tests. Errors are greatest at the beginning of the cycle, with a maximum error of 0.5 °C for 0.22 l·s^{-1} and 0.56 °C for 0.32 l·s^{-1}. Thus, for the purposes of the current work, the results of this validation are considered acceptable. The model performs particularly well during latent heat transfer and after charging is complete. The discrepancies at the beginning of the process can possibly be attributed to a greater thermal inertia in the experimental setup. Figure 6 compares the heat transfer rate across the tank from the model with the experimental results from Liu et al. (0.22 l·s^{-1}). Figure 7 compares the cumulative heat transfer, summed every 30 minutes for the experimental and modelled cases (0.22 l·s^{-1}). The difference between the predicted and experimental total heat transfer across the thermal storage unit is within 1% and 2.5%, for the 0.22 l·s^{-1} and 0.32 l·s^{-1} tests, respectively.

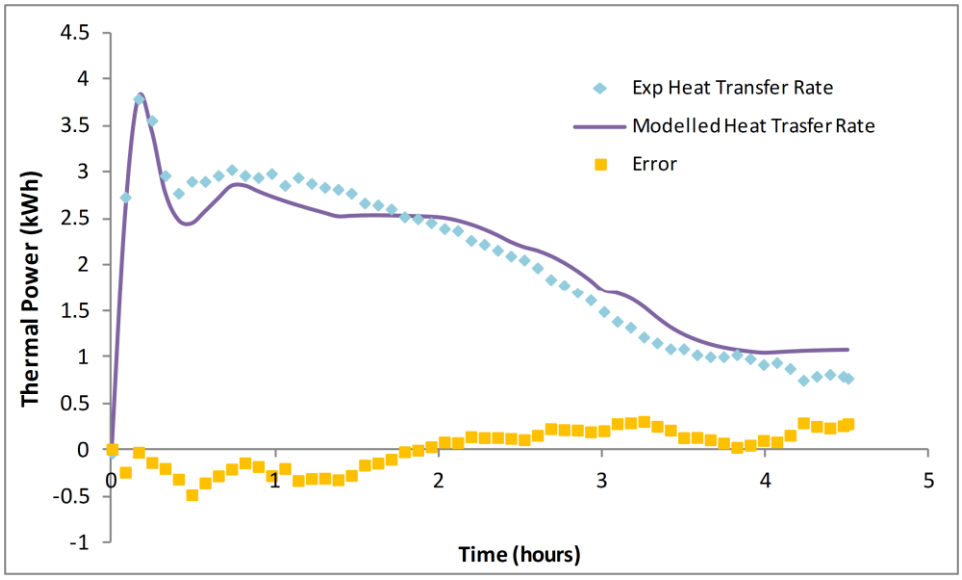

Figure 6: Modelled versus experimental heat transfer rate (0.22 l·s^{-1})

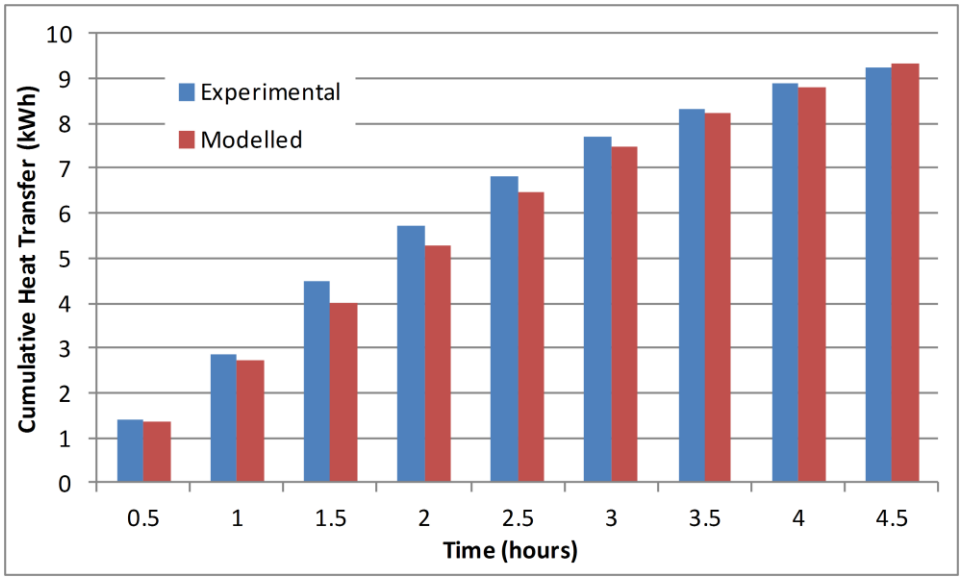

Figure 7: Modelled versus experimental cumulative heat transfer (0.22 l·s^{-1})

5 Simulation Procedure

To assess the impact of using the TES device on the system performance, a preliminary storage strategy was analysed using the building simulation environment and compared against a reference base case over a 24 hour period. A day of moderate heating load was chosen, so that the thermal storage tank would be fully utilised. The peak time was chosen to be from 07:00 to 21:00, with off-peak being all times outside of this. Occupancy hours are considered to be 07:00 to 19:00; this entire period is considered to be on-peak

Base Case

The base case for this analysis is the GSHP system meeting the building heating load directly, without any thermal storage intervention. Indoor temperatures are allowed to float outside of occupancy hours. During occupied times, the constant setpoint temperature is 22 °C is maintained by the variable speed fan coil units. A water return setpoint temperature of 35 °C (Figure 2, T_1) is used on the building side of the GSHP; a water temperature deadband of 1 °C is used about this setpoint. The internal primary and secondary pumps operate with a fixed mass flow rate of 2 kg·s^{-1} between 07:00 and 19:00; the external circulation pump cycles on and off with the GSHP.

Inclusion of Thermal Storage

To analyse the impact of utilising the thermal storage, a simple strategy is used wherein the GSHP operates to fully charge the PCM tank during off-peak hours. Under the storage strategy, the primary circulation pump is constantly operational through the hours of 00:00 to 19:00. All of the water from this pump (2 kg.s^{-1}) flows through the TSU. Thus, the TSU absorbs heat when the GSHP is in charging mode and when heat is required by the secondary loop, the water flows through the TSU to discharge. Once the TSU is depleted, (the primary outlet temperature (Figure 2, T_2) drops below 42 °C: see Figure 8), all further water flow bypasses the storage tank and the GSHP cycles on to meet the load. The GSHP is set to charge the TSU during the hours of 00:00 to 07:00; the external circuit pump cycles on and off with

the GSHP. The secondary circuit pump is operational from 07:00 to 19:00. Fan coil units in the rooms are scheduled off during unoccupied times and have variable air flow during the hours of operation, with a setpoint temperature of 22 °C.

Two set-points are used on the return side of the GSHP: 50°C when charging the TSU and 35°C when operating during peak hours. A deadband of 1 °C is used. Under this strategy, use of the GSHP is minimised during on-peak hours: the PCM tank is discharged fully before the GSHP becomes operational. As seen in Figure 8, the primary circuit outlet temperature cycles frequently with the GSHP between 00:00 and 03:00, and then from 14:00 to 19:00. This represents the simplest form of charge-discharge mechanism.

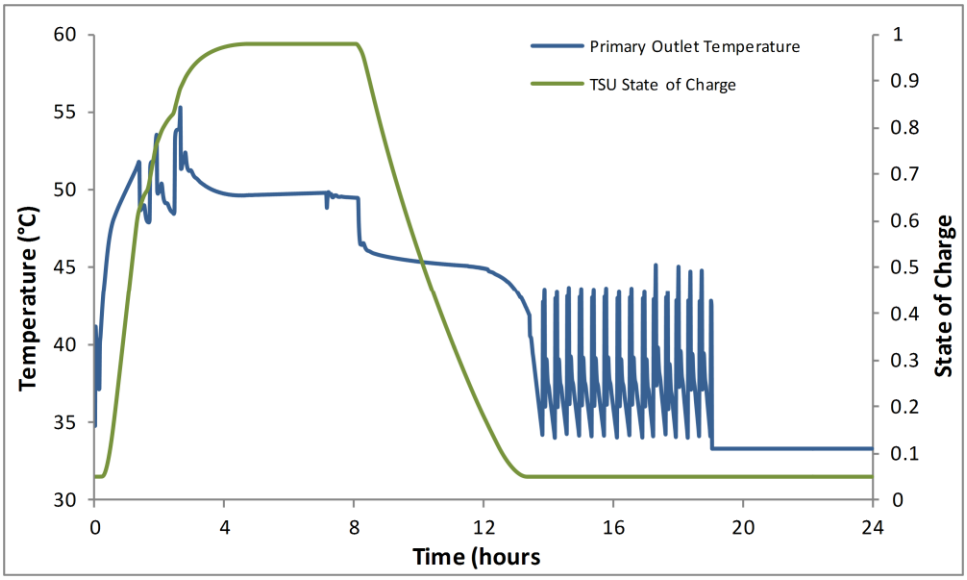

Figure 8: Storage strategy, primary circuit outlet temperature and TSU state of charge

6 Results

The base case and thermal storage strategy were simulated as described above. The effects on the energy consumption and system performance are outlined in this section. The use of thermal energy storage would typically result in increased energy consumption. Here the impacts on the individual components are detailed, as well as the seasonal performance factor when including different system components.

Energy Analysis

Energy consumption is contrasted with that for the base case in Table 2. The external pump is relatively unaffected. The internal primary pump has a higher consumption (2.14 kWh vs 1.34 kWh) as it must be on during the time taken to charge and discharge the TSU. The secondary pump is largely unaffected, as it operates for the same period in both cases. Fan power consumption is seen to decrease (10.95 kWh vs 12.56 kWh) because of the higher water temperature supplied to the fan coils from the primary circuit when discharging the tank, increasing the fan coil capacity and requiring a lower air mass flow rate to meet the space load. The GSHP power consumption is increased, as the GSHP performance decreases with higher supply water temperatures needed to charge the PCM TSU, as seen in Figure 9.

Table 2: Storage strategy versus base case - energy consumption

Component	Energy Use (kWh) Base Case	Energy Use (kWh) Storage Strategy
GSHP	40.49	47.29
External Pump	0.55	0.55
Primary Pump	1.34	2.15
Secondary Pump	5.33	5.38
Fans	12.56	10.95
Total	**60.26**	**66.32**

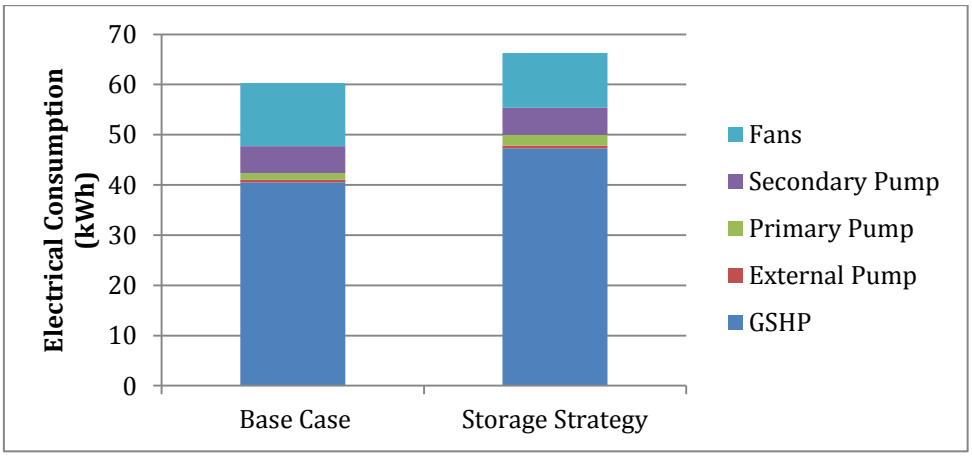

Figure 9: Energy consumption for base case and storage strategy

System Performance

The seasonal performance factor (SPF) is defined for this work as the ratio of heat load delivered to electrical input as in Equation 4 over the 24 hour period. The power consumption considered for each of SPF_1, SPF_2, SPF_3 and SPF_4 are defined in Table 3. The use of different SPFs allows for performance of different parts of the GSHP system. SPFs are compared for the storage strategy against the base case in Figure 10.

$$SPF = \frac{\int_0^{24} \dot{Q}_{GSHP} \, . \, dt}{\int_0^{24} P \, . \, dt} \tag{4}$$

Table 3: Power consumption by SPF

SPF number	Power Consumption Considered
SPF_1	GSHP
SPF_2	GSHP + external pump
SPF_3	GSHP + external pump + internal pumps
SPF_4	GSHP + external pump + internal pumps + fans

Figure 10: SPF_{1-4} for base case and storage strategy

Load Shifting

The on-peak energy use is contrasted against that used during the off-peak hours and is shown in Table 4. Figure 11 shows the electrical load averaged over consecutive 30 minute periods, demonstrating the change in electrical load profile. The loads are averaged for clarity, but it should be noted that this process has removed the transience associated with the GSHP cycling. Most of the GSHP power consumption has been shifted to off-peak hours through use of this strategy. The primary circuit pump on-peak consumption is relatively unaffected; the extra 0.79 kWh is consumed off-peak. By its nature, fan power consumption is entirely on-peak, as is the secondary pump, as Figure 12 shows, most of the pump power remains on-peak.

Table 4: Peak versus off-peak electricity consumption (kWh)

	Base Case Off-Peak	Base Case On-Peak	Storage Strategy Off-Peak	Storage Strategy On-Peak
GSHP	0	40.49	31.82	15.47
External Pump	0	0.55	0.34	0.21
Primary Pump	0	1.34	0.79	1.36
Secondary Pump	0	5.33	0	5.38
Fans	0	12.56	0	10.95
Total	**0**	**60.26**	**32.95**	**33.37**

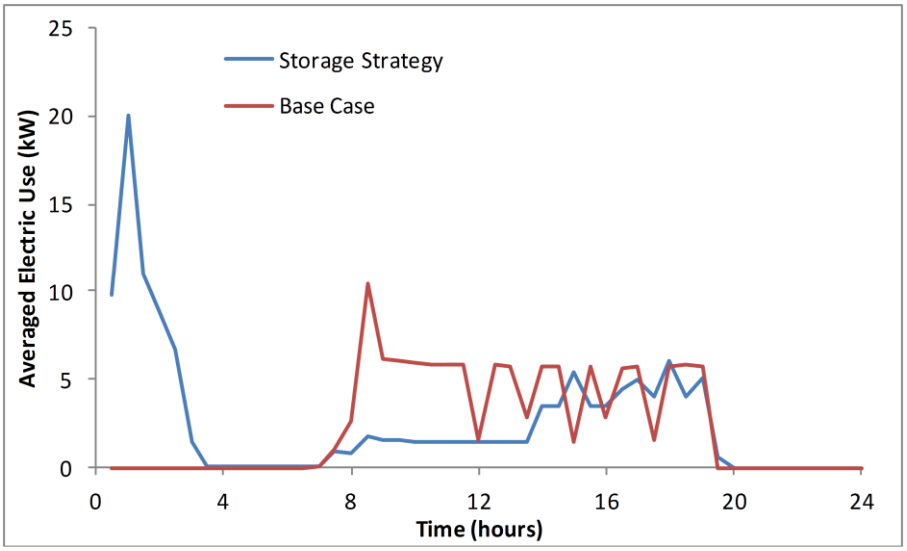

Figure 11: Electrical load profile: base case and storage strategy averaged every 30 mins

While a heating load shift of 100kWh is achievable, the electrical load shift is of greater interest. The high COP and associated SPF of this heat pump mean that electrical load shifting is substantially less than the 100 kWh thermal energy stored. The on-peak electrical load is reduced from 60.27 to 33.61 kWh – approximately half. There is a penalty for this load shifting: a 6.04 kWh or 10% increase in daily electricity consumption. The purpose of thermal energy storage is not for local energy saving, but for demand management. The incentive used to encourage demand shifting is typically monetary. Instances in the literature suggest a peak to off-peak tariff of up to 2:1 and 4:1 (Hajiah and Krarti, 2012b; Henze et al., 2004). To offset this added cost, energy consumed off-peak would need to be discounted by 18.5% for the storage strategy energy cost to equal the energy cost for the base case charged at a flat rate. Thus, under a more heavily incentivised structure, substantial cost savings would be made.

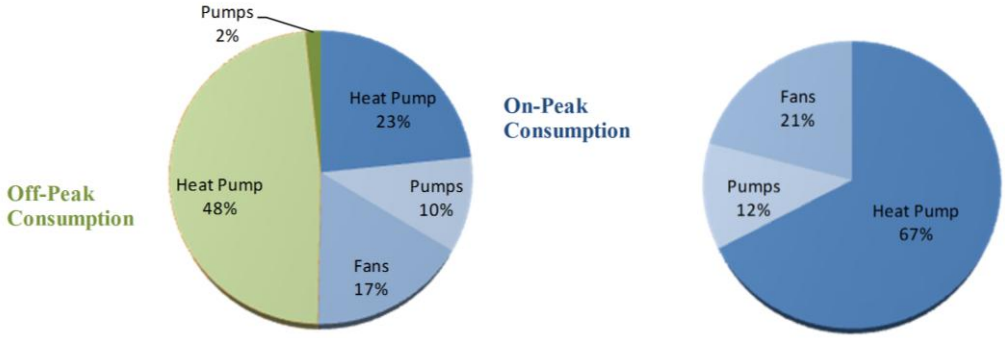

Figure 12: Electricity consumption (a) storage strategy on and off-peak (b) base case

7 Discussion

Heating load shifting is a real possibility using a PCM thermal storage unit such as that presented in this paper. 49% of the electricity associated with heating loads for this day was moved to off-peak hours (for the case of storage being used). The times chosen as peak or off-peak can be changed according to the needs of the grid; this is what brings such flexibility to the load management and is the main reason for using this technology. It is not as straightforward as suggesting that the electricity shifting potential is solely dependent on the capacity of the storage tank. What must be considered is the performance of the system as a whole, including the primary and secondary circuits as follows:

Primary Circuit: There is a significant penalty for using this thermal storage unit, largely due to the diminishing performance of the GSHP at higher temperatures. The GSHP power consumption increases by 16%. This is an inherent compromise due to the fact that the heat is stored at a higher temperature than the usual setpoint temperature. To charge this storage unit, the melting point must be exceeded by the GSHP supply temperature, decreasing the GSHP performance and increasing power consumption. The primary pump also operates for longer, further increasing power consumption.

Secondary Circuit: Through use of the active thermal store, the fan power consumption cannot be shifted in this way, nor can the power consumed by the secondary pump. The power consumption of the secondary pumps was largely unchanged as it only operates to deliver the load directly to the zones. An unexpected energy saving was seen in the fan coil units. From Figure 8, it can be seen that the supply water temperature coming from the primary circuit is higher than that supplied by the GSHP under normal operation. Thus, the heating capacity of the water is higher, leading to a decrease in fan power required.

Considering the whole system, electricity consumption is increased by 10%. The increase in energy consumption can be justified by utilities in terms of the demand side management and the ability to shift building load away from peak times. For such a strategy to be adopted by operators of commercial buildings, a price incentive would have to be introduced. To break even in this scenario, off-peak prices would have to be reduced by 18.5%. Thus a ratio of 2:1 would be more than sufficient to result in substantial reduction in building running costs.

8 Conclusions

A validated model of a heating PCM thermal storage unit is presented in this paper, as is its integration into the EnergyPlus building simulation environment. Two cases were presented: one with no thermal storage present and one with a 100 kWh (thermal) PCM TSU present. The energy consumption for both cases was compared, showing an increase of 10% increase in total energy consumption over a 24 hour period. On-peak electricity consumption was reduced by 44% through this use of this strategy. A minimum off-peak electricity cost reduction of 18.5% would be needed for this case to be financially viable to the building operator, which is realistic, given the flexibility of supply that is added to the building load.

9 Nomenclature

Acronyms

BCVTB	Building Controls Virtual Test Bed
GSHP	ground source heat pump
HTF	heat transfer fluid
PCM	phase change material
TSU	thermal storage unit
SPF	seasonal performance factor
COP	coefficient of performance

Symbols

A	area	(m^2)
D_h	hydraulic diameter	(m)

k	thermal conductivity	$(W \cdot m^{-1} \cdot K^{-1})$
Nu	Nusselt Number	
P	power	(W)
Pr	Prandtl Number	
$\dot{Q}$	heat transfer rate	(W)
Re	Reynolds Number	
t	thickness	(m)

10 Acknowledgement

This research is funded by the European Union through the GroundMed FP7 project (www.groundmed.eu). The cooperation of those at ISR-University of Coimbra Coimbra is appreciated, in particular Professor Anibal De Almeida.

11 Bibliography

Choi, C.Y., Hsieh, C.K., 1992. Solution of Stefan problems imposed with cyclic temperature and flux boundary conditions. International Journal of Heat and Mass Transfer 35, 1181–1195.

D'Avignon, K., Kummert, M., 2012. Proposed TRNSYS Model for Storage Tank with Encapsulated Phase Change Materials. Presented at the SimBuild, IBPSA, Wisconsin, 423-430.

Elsayed, A.O., 2007. Numerical study of ice melting inside rectangular capsule under cyclic temperature of heat transfer fluid. Energy Conversion and Management 48, 124–130.

Hajiah, A., Krarti, M., 2012a. Optimal control of building storage systems using both ice storage and thermal mass – Part I: Simulation environment. Energy Conversion and Management 64, 499–508.

Hajiah, A., Krarti, M., 2012b. Optimal controls of building storage systems using both ice storage and thermal mass – Part II: Parametric analysis. Energy Conversion and Management 64, 509–515.

Henze, G.P., Felsmann, C., Knabe, G., 2004. Evaluation of optimal control for active and passive building thermal storage. International Journal of Thermal Sciences 43, 173–183.

Henze, G.P., Krarti, M., Brandemuehl, M.J., 1997. A Simulation Environment for the Analysis of Ice Storage Controls. HVAC&R Research 3, 128–148.

Ihm, P., Krarti, M., Henze, G.P., 2004. Development of a thermal energy storage model for EnergyPlus. Energy and Buildings 36, 807–814.

Jones, A., Finn, D., 2013. Ground Source Heat Pump Modelling with Thermal Storage - Simulation and Integration Issues in EnergyPlus. Presented at 13th Conference of IBPSA, Chambéry, France, August 26-28, 2916-2923

Kintner-Meyer, M., Emery, A.F., 1995. Optimal control of an HVAC system using cold storage and building thermal capacitance. Energy and Buildings 23, 19–31.

Liu, M., 2010. Development of a Phase Change Thermal Storage Unit for Refrigerated Trucks. PhD Thesis, University of South Australia.

Liu, M., Saman, W., Bruno, F., 2011. Validation of a mathematical model for encapsulated phase change material flat slabs for cooling applications. Applied Thermal Engineering 31, 2340–2347.

Shah, R.K., London, A.L., 1978. Laminar flow forced convection in ducts : a source book for compact heat exchanger analytical data. Academic Press, New York, ISBN 0120200511.